# Optimizing Impact Properties of PP Composites by Control of Spherulitic Morphology

**Y. S. ISMAIL,[1] M. O. W. RICHARDSON,[1] R. H. OLLEY[2]**

[1] Institute of Polymer Technology and Materials Engineering, Loughborough University, Leicestershire LE11 3TU, United Kingdom

[2] J. J. Thomson Physical Laboratory, Whiteknights, Reading RG6 6AF, United Kingdom

*Received 31 December 1999; accepted 20 May 2000*

**ABSTRACT:** The objective of this work was to investigate methods for increasing the impact resistance of composite sheets made from glassfiber mat–reinforced polypropylene prepeg by varying its thermal history. A 60:40 (wt %) mixture of woven glass fiber–PP was crystallized at various temperatures and times to examine the effect of the thermal history (during cooling from the melt) on the degree of crystallinity and spherulitic morphology and to study the relationship between these factors and mechanical properties. The composite laminates were manufactured within a flat mold using a compression molding press and then crystallized from the melt in the range 106–156°C for 10, 30, 60, and 240 min in an air oven. The degree of crystallinity that developed in the matrix polymer was determined using differential scanning calorimetry (DSC), and the matrix morphology was examined by permanganic etching followed by scanning electron microscopy. The highest peak and failure energies during impact were achieved when maximum crystallinity was produced in the specimen crystallized at 134°C for 4 h. Electron microscopy of etched interior sections of impacted specimens has enabled a more detailed understanding of the impact behavior of these materials. The greatest improvement appears to result from an increase in the propensity of cracks to propagate along spherulitic boundaries by virtue of mechanisms facilitated by the results of the differential contraction of the crystalline and amorphous phases within the polypropylene. Differential contraction of the glass and polypropylene appears to be a less important factor, although voids created by such processes have to be taken into account. © 2000 John Wiley & Sons, Inc. J Appl Polym Sci 79: 1704–1715, 2001

**Key words:** Key words: impact energy; composites; polypropylene spherulites; etching

## INTRODUCTION

In recent years there has been rapid growth in the use of fiber-reinforced composite materials in engineering applications, and there is every indication that this will continue. In particular, fiber-reinforced thermoplastic composites are being widely used in various applications ranging from leisure or sports equipment to heavy and advanced engineering applications such as those associated with the automobile, aircraft, and even the aerospace industries.

Increasing interest in thermoplastic-based composites has occurred because of their economic and technical advantages, such as ease of fabrication, environmental friendliness, greater toughness, recyclability and rapid fabrication cycle.[1] Particular advantages have been found with

*Correspondence to:* R. H. Olley (r.h.olley@reading.ac.uk).

Journal of Applied Polymer Science, Vol. 79, 1704–1715 (2001)

the emergence of a variety of new manufacturing techniques that allow processing with long or continuous fibers.[2,3] Long-fiber composites show significant advantages in impact properties as compared with short-fiber composites,[4] but where possible the greatest advantages are found in continuous fiber composites made from woven fiber mats called prepregs, which offer ease of fabrication and an almost indefinite shelf life. In addition to these advantages, their useful mechanical and physical properties (though not always as great as those of thermoset composites) are playing an important role in extending applications even farther. Unlike metals, most properties of thermoplastic polymeric composite materials are a complex function of a number of parameters such as shape, size, orientation, and distribution of the reinforcement and the mechanical properties of the matrix, which are affected by a number of variables including degree of crystallinity, size, and number of spherulites, all of which are greatly affected by cooling rates and thermal histories (temperatures, times, and pressures) during and after processing. In some cases, when fibers are embedded in a molten thermoplastic, they may act as a nucleant so that transcrystallinity will form close to the glass interface.

It is possible to take a simplistic approach and to relate the mechanical properties (tensile, compressive, shear, and fracture toughness) to the degree of crystallinity, as has been done for polyether-ether-ketone (PEEK) and its composites.[5] However, the problem of relating crystallinity and mechanical properties has not been fully and precisely solved: in practice, the simple measure of crystallinity is inadequate, and it may be necessary to take into account size, shape, and perfection of both crystals and spherulites.

It has generally been observed in semicrystalline polymers that slower cooling results in larger spherulites along with a greater degree of crystallinity. For polypropylene it was found that the impact strength, elongation at break, Young's modulus, and yield stress all decrease as the spherulite size increases.[6,7] Studies of glass–PP laminate show that the slowest cooling rates give rise to higher-impact energy materials than those produced by intermediate or fast cooling rates. Cracks easily propagate through the slowest-cooled material because of interspherulitic defects, giving to this material the highest low-velocity impact resistance.[8] Similar effects in relation to spherulite size and degree of crystallinity are observed in relation to the interlaminar fracture toughness (Modes I and II) of commingled yarn-based glass fiber–PP composites.[9]

Residual stresses may affect the mechanical properties. In a study of the influence of stamping temperature on the properties of a glass-mat thermoplastic composite,[10] it was found that impact strength (from Charpy and drop-weight tests) increases with increasing mold temperature and the Charpy impact strength improved significantly with further heat treatment of the samples. It is believed that the use of a lower mold temperature results in the generation of greater residual stresses because of the faster cooling rates involved; however it seems that at a higher stamping temperature, the residual stresses should be less because there is more time for material relaxation.

Some fibers when embedded in a thermoplastic melt may also act as a nucleant for the growth of spherulites. If there are many nucleation sites along a fiber's surface, then a columnar growth known as transcrystallinity will develop and enclose the fiber, but its extent will be restricted by the growth of neighboring spherulites.[11] Although the geometry of the transcrystalline layers is different in spherulites, they are otherwise similar in terms of crystallography and lamellar architecture, and they have the same outward growth rates and dimensions.[12,13] They can be regarded as a special case of spherulites grown from massed nuclei lying in a single plane or on a curved cylindrical surface, and in this they differ from row nuclei, which have correlated crystallography with all lamellae initially sharing a common *c*-axis.[14] It has been proposed[15] that the origin of transcrystallization is actually stress-induced nucleation from the stresses caused by cooling two materials in close proximity, which exhibit a large difference in the thermal expansion coefficient. If transcrystallization is related to such stresses developed at the fiber–melt interface, then one of the factors influencing the occurrence of transcrystallization should be the cooling rate. Further stress may develop on cooling after crystallization as a result of thermal expansion coefficient mismatch between the fibers and the transcrystalline layer.[16] In addition, the mechanical properties of the transcrystalline layer may differ from those of the spherulitic material.[17] However, transcrystallinity is not always observed in PP–fiber composites.[8]

In this work a series of specimens prepared with systematic variations in crystallization temperature and time were examined in order to optimize the conditions for their preparation and to

correlate the observed mechanical properties with variations in spherulitic morphology produced by the various treatments.

## EXPERIMENTAL

### Materials

The raw material, Twintex TPP, Vetrotex International, Chambery, France, consists of commingled E-glass and polypropylene fibers woven into a bidirectional cloth. The volume fraction of glass fibers is 0.34, and the melt flow index (MFI) is 8.7 g/10 min.

### Preparation of Laminate Sheets and Specimens

Sheets of Twintex TPP were cut and tailored to the mold size (approximately 150 mm × 150 mm and 2.5 mm thick) and six layers of cloth were placed into a flat mold, which was covered with a 200 mm × 200 mm sheet of poly(ethylene terephthalate) (PET) sheet, and two flat plates measuring 200 mm × 200 mm and with a thickness of 2.5 mm were placed on the top and bottom of the mold. Then the flat mold (held by these two flat plates) was placed into a heated press and allow to preheat up to 190°C, without pressure. At 190°C (above the melting temperature of PP), an approximate pressure of 5 tons on a 10-cm-diameter ram was applied for 10 min.

In order to produce a series of glass fiber–reinforced PP laminates systematically varied in terms of crystalline structure, only the thermal history of specimens was varied; kept constant were all other processing conditions, such as geometric of lay-up and number of plies, thickness, pressure, and temperature. Several heat treatments were used to vary the morphology of these laminates as follows:

After pressing, the samples were immediately transferred to a convective-type (hot-air fan-driven) oven, a size-2 Gallenkamp Hot-Box oven. The samples were crystallized in this oven at temperatures in the range 106–156°C and four crystallization times were applied—10, 30, 60, and 240 min—then the samples were immediately quenched in cold water.

### Preparation of Samples for Microscopy and Etching

Samples measuring 20 mm × 20 mm with a thickness of 2.5 mm were placed upright in a plastic mount 30 mm in diameter and 25 mm tall. In order to prevent the samples from tumbling when pouring the epoxy resin, plastic clips were fixed at the bottom sides of the samples. The epoxy resin was Araldite MY 750 combined with Araldite Hardener HY (Ciba Speciality Chemicals, Vantico Ltd., Cambridge, UK) 951 at a ratio 10:1. After pouring the resin, the mount was immediately transferred into a vacuum pump for 2–3 h in order to release air bubbles trapped in the resin. The curing time was 15–20 h.

The surface of the samples to be etched or examined under the microscope were ground using 420-grit silicon carbide paper followed by 600-grit aluminum oxide paper, with water lubrication to prevent overheating. The surface was further polished by using a 6 $\mu$m diamond suspension with a polishing wheel speed of 350 rpm. After coarse scratches were removed, the final polishing was completed by using a 1 $\mu$m diamond suspension. Finally, the samples were washed with running tap water and detergent and quick-washed with acetone before being dried with a hair dryer.

### Etching

The improved permanganic etching technique[18] employs potassium permanganate in concentrated sulfuric acid and orthophosphoric acid, but here some modification has been made to the original acid mixture by the addition of distilled water to allow for the polypropylene and epoxy resin to be etched at comparable rates.

The acid mixture used was prepared by mixing in this order: 2 vol distilled water, 2 vol orthophosphoric acid, 5 vol concentrated sulfuric acid. The mixture was allowed to cool before adding 1 g potassium permanganate powder per 100 mL of etchant, which was poured through a glass funnel into the conical flask containing the acid mixture as it was being stirred using a magnetic stirrer at high speed, a process continued for 30 min to ensure complete dissolution of the potassium permanganate. Then the sample (prepared in a mount as explained in the Preparation of Samples for Microscopy and Etching section) was placed in 125 mL of etchant in a 180-mL wide-mouth glass bottle with a PP cap. The samples were suspended (floated) with the polished surface downward and gently agitated in an alternating shaker for 1 h.

After the shaking treatment, a quenching mixture of 1 part 30% hydrogen peroxide to 9 parts precooled mixture of 2 parts conc. sulfuric acid to 7 parts water was gently poured down the side of the bottle and to stop the reaction and to get the

mount/specimen to float up. Then the mount/specimen was placed in a beaker with some dilute quenching mixture to ensure that all the brown deposit of manganese dioxide was dissolved. The mount/specimen was washed once with distilled water before being soaked in a Jeyes Bloo solution (a proprietary cleaning agent) for 1 h. Finally, the specimens were washed 3 times with distilled water and then quick-washed with methanol before being allowed to dry.

### Differential Scanning Calorimetry

In semicrystalline thermoplastic-based composites, crystalline features such as degree of crystallinity are important parameters effecting the mechanical properties. Degree of crystallinity, in turn, is influenced by the cooling rate and thermal histories of the samples.

In this study differential scanning calorimetry (DSC) with a DSC 10 differential scanning calorimeter (TA Instruments Ltd.) was used to determine of the degree of crystallinity ($\chi$) and melting temperature ($T_m$) of all the prepared samples. The specifications of the 990 thermal analyzer were as follows—program mode: heat; atmosphere: nitrogen gas; sample weight: approximately 10–- 15 mg; time base: none; calibration: indium; temperature range: 20–200°C; heating rate: 10°C/min.

The degree of crystallinity of samples was calculated as follows:

$$\chi = 100 \times (\Delta Hf_s/\Delta Hf_{100}) \times 100/\%\text{PP}$$

where $\Delta Hf_s$ is the heat of fusion of the sample and $\Delta Hf_{100}$ is the heat of fusion of a hypothetical 100% crystalline sample, and % PP is the wt % of PP from a burn-off test, to correct for the mass of glass fiber in the sample. In this study the heat of fusion of hypothetical 100% crystalline polypropylene was taken as 209 J/g.[19]

### Instrumented Falling-Weight Impact Testing of Specimens

Impact testing of the specimens was done at room temperature (20°C). To produce the specimens for the impact test, laminate sheets were cut to 65 mm × 65 mm. A Rosand Instrumented Falling Weight Impact (IFWI) tester was used throughout. The specimens were clamped ,and the test was repeated 6–8 times for each condition to produce an average figure. This system allows the setting of certain pretest parameters, and those adopted for the current work were: mass 26.2 kg; sweep time 10 ms; delay 10; range 10 kN; velocity 3 m/s; filter frequency 1000 Hz.

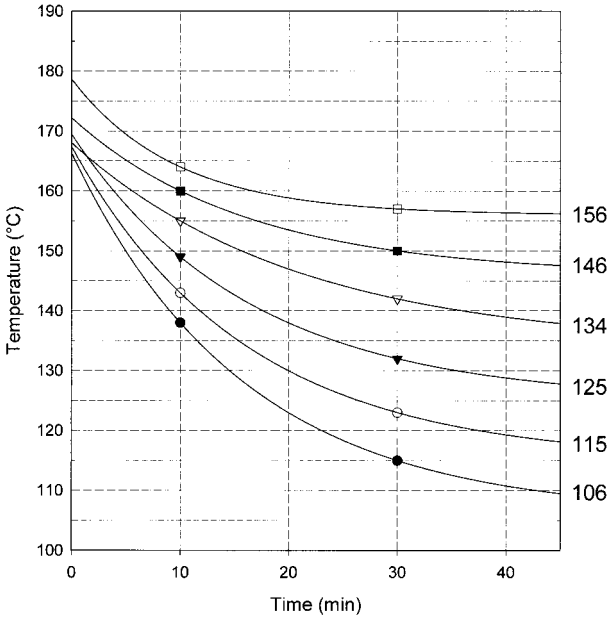


**Figure 1** Cooling of specimens in the oven during crystallization procedure and fitted exponential cooling curves.

## RESULTS AND DISCUSSION

### Thermal History

An explanation of the changes in specimen impact performance (as spherulitic and transcrystalline morphologies vary) can be sought in the differences in impurity segregation, contraction during and after crystallization, formation of voids, and interfacial bonding between the transcrystalline layers and the glass fibers (arising from different thermal histories during crystallization in the oven). To account for these developments, it is necessary to examine these thermal histories more precisely.

After the specimens in their molten state (190°C) are transferred from the press to the crystallization oven, attainment of the desired crystallization temperature is a slow process. Cooling curves (Fig. 1) are estimated from readings after 10 min and 30 min and assume exponential decay according to Newton's law of cooling, but allow for cooling during the transfer. The lack of a good fit at lower temperatures suggests the oven may operate less effectively at low temperatures. Those specimens being cooled to 106°C will cool the fast-

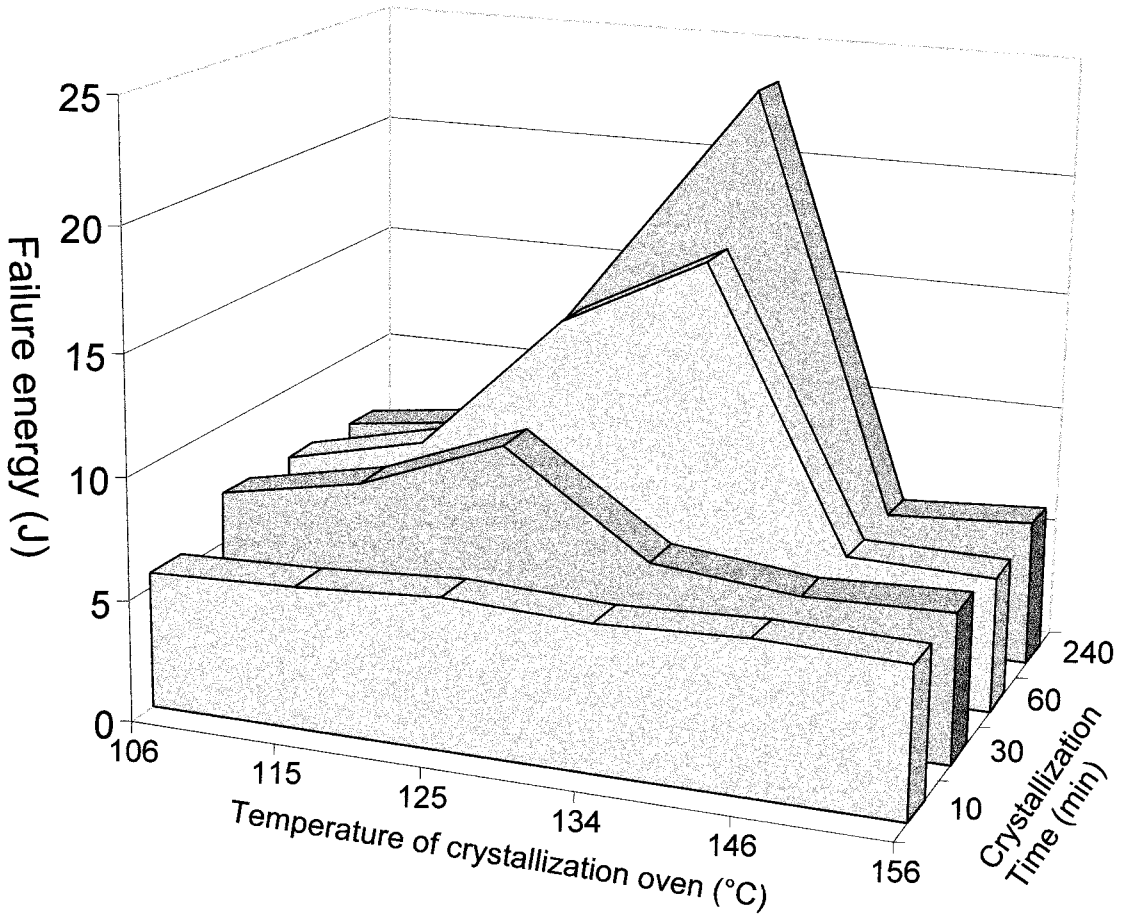


**Figure 2** Development of failure energy as a function of crystallization temperature and time.

est, but after 10 min even these have only cooled to 138°C, a temperature at which crystallization will have hardly begun. It is therefore not surprising that none of the 10-min specimens possess a high value of failure energy (Fig. 2). After 30 min the 125°C specimen exhibits the highest energy. All three treatments—106°C, 115°C, and 125°C—have now entered a temperature region at which crystallization can take place, but the last of these has spent a longer time at a somewhat higher crystallization temperature, in excess of 130°C. Only after 1 h does the 134°C treatment overtake the 125°C treatment, but both of these continue to show improvement up to 4 h. One can therefore define three time zones: the *pre-crystallization* period, while the material cools to a temperature at which crystallization can begin; the *crystallization* period, from nucleation to space-filling spherulitic growth; and the *maturation* period, during which further changes take place. In consequence, the observed behavior is not expected to show a simple bivariate dependence on crystallization temperature or time. Instead, it can pass through stages where either the material shows only rapid crystallization on quenching after removal from the oven, or else slower crystallization, which may be effectively isothermal or nonisothermal, depending on where on the cooling curves it takes place, followed by annealing, which continues after the volume of the PP has filled with spherulites.

Microscopy results will be evaluated in detail later, but a simple measure of spherulite sizes associated with the 4-h specimens is shown in Figure 3. It is also evident from these that the 146°C and 156°C specimens were still completely molten after this time, while all the lower-temperature specimens were completely crystallized. It would be expected, both on theoretical grounds[20] and from experience, that there would be a roughly exponential increase in spherulite size with $T_c$, but this is not observed. From such considerations and from the known growth rates of PP spherulites,[21] it would appear that the

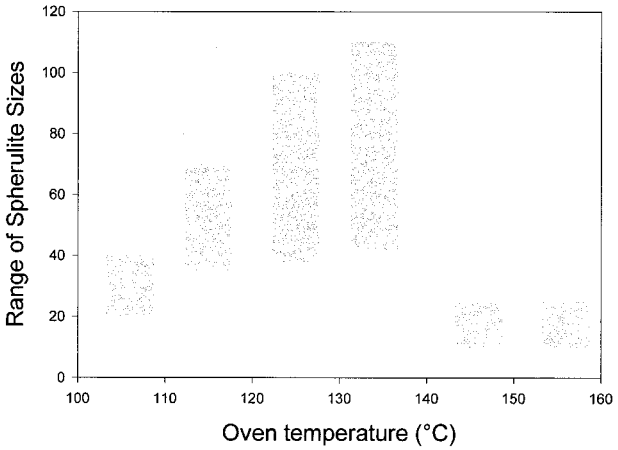


**Figure 3** Range of spherulite sizes in 240-min specimens.

106°C specimen actually crystallized at 115°C or greater during cooling, while in a similar way the 115°C and 125°C specimens have crystallized nearer to 130°C.

## Impact Testing

The peak and failure energies for all specimens are plotted in Figure 4. The peak energy is the energy under the force-deflection curve up to peak force, in which initiation of damage occurs in the specimen, and failure energy is the energy under the force-deflection curve up to peak deflection where propagation of damage takes place until fracture. The failure energy values are simply a replot on a different basis of the values shown in Figure 2, but the peak energies are also seen to follow the same trends. It can be seen that in general all samples treated for 10 min, as well as those held in a molten state at higher temperatures (146°C and 156°C) have low values of peak and failure energies, that is, in the range of 3–6 J, and this figure can be said to correspond to quenched or rapidly cooled PP. However, even a small increase in crystal perfection brought about by slower crystallization is significant, for example in the 30-min 106°C, 115°C, and 125°C specimens, where a slight increase in the peak and failure energies can be seen, indicating crystallization in the oven has at least begun, in contrast to the higher temperatures, up to 156°C, where the peak and failure energies remain the same after 10 min. When the crystallization time was increased to 1 h or 4 h, there was a much more significant increase in the peak and failure energies of the 125°C and 134°C samples, with the highest peak and failure energies in the sample crystallized at 134°C for 4 h, that is, 14.9 J and 23.3 J, respectively. It will be seen that the propagation of damage after impact is also more extensive in these 134°C specimens.

## Spherulitic Morphology

The general structure of the compressed specimens can be seen in the micrograph of specimen A at low magnification in Figure 5, in which the individual sheets have been molded together. However, two glass-fiber weaves are sometimes found with one sheet in register with its neighbor and sometimes with it out of register. Note should be taken of the foreshortening of the view by sample tilting, manifested in the elliptical appearance of the supporting plugs, which are actually circular in section. The variation of spherulite size can be followed at a higher magnification in three specimens crystallized to completion for 4 h, at 106°C, 115°C, and 125°C. The size of the

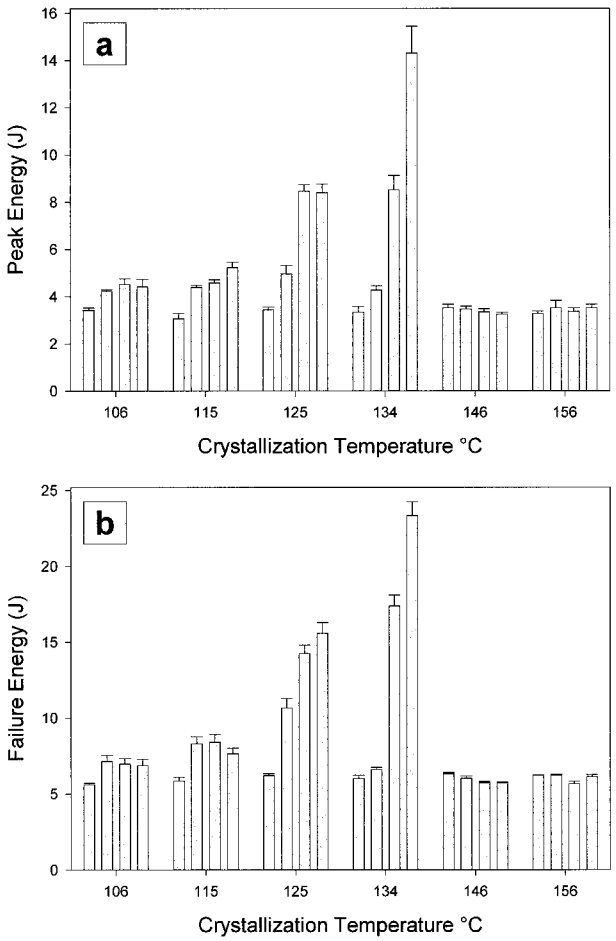


**Figure 4** Peak energy (a) and failure energy (b) for all specimens.

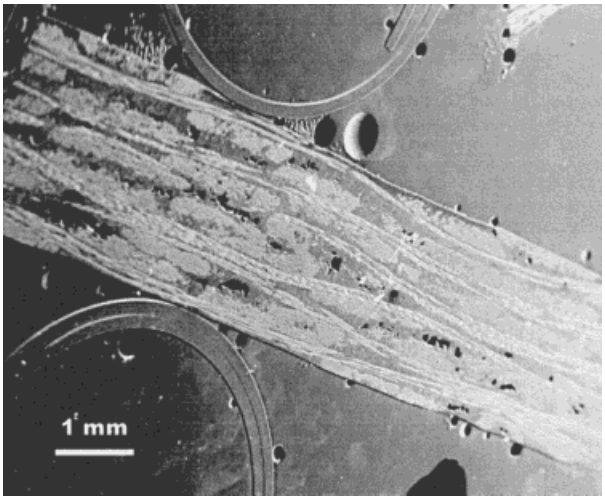


**Figure 5** SEM micrograph at low magnification showing the general structure of the compressed specimen in a sample crystallized at 106°C for 240 min.

spherulites in PP varies greatly with crystallization temperature, as nucleation becomes several time more dense with every 10°C drop in $T_c$. This can be followed by looking first at the specimens crystallized for the maximum time of 240 min. At 106°C [Fig. 6(a)] the spherulites are rarely greater than 20 $\mu$m in diameter, at 115°C [Fig. 6(b)] they are much larger, often greater than 70 $\mu$m in diameter. The spherules would be expected to be significantly larger in the 125°C specimen [Fig. 6(c)], but they are only slightly larger, up to 100 $\mu$m in diameter. On examination of the cooling curves in Figure 1, in accord with the known growth rates of polypropylene spherulites, the spherulites in the 125°C specimens actually form at a few degrees in excess of 130°C. In the 115°C specimen the faster cooling would have brought the specimen close to 130°C when crystallization occurred, and in the 106°C specimen, at about 125°C. The largest spherulites, ranging from 40 to 110 $\mu$m, are seen in the 134°C specimen, to be discussed in greater detail next [Fig. 7(d)]. The very smallest spherulites are found at 145°C, and at 156°C as seen in Figure 6(d), so crystallization is understood to have occurred during the much more rapid cooling after the specimen was removed from the oven.

The slow attainment of crystallization temperature is much more apparent in the 134°C specimens. In the 10-min specimen [Fig. 7(a)], the spherulites are roughly the same size as the 156°C 240-min specimen in Figure 6(d). Here again the sheet was still entirely molten after 10 min, and all the spherulites had formed as the sample was rapidly cooled after removal from the oven. After 30 min [Fig. 7(b)], it is possible to see some spherulites (arrowed) that have started to grow in the oven, but a steplike discontinuity in the spherulites is also seen, formed when the sheet was taken out and cooled, and the morphology of the continued radial growth became finer and is more heavily etched. After 60 min [Fig. 7(c)] growth is practically complete, but areas can still be seen where melt has remained at the end of the treatment, and the corresponding step is visible in the transcrystalline layer (arrowed) as well as in the spherulites. An additional feature is seen in the specimen crystallized at 134°C for 4 h [Fig. 7(d)]. Here the spherulites have filled the specimen long before treatment was complete, and cracks are seen between their boundaries. Although these cracks were probably extended or deepened by the etching,[22] they were present in the original specimen. On examining impacted specimens under an optical stereomicroscope, it was possible to see that such cracks had been opened further by the impact, not only in the domed regions (characteristic of these specimens after impact) but extending further into apparently undeformed regions [Fig. 7(d)].

It can be seen in Figure 6(a–c) that transcrystalline layers formed around many of the fibers in several specimens, but there is no systematic variation in the occurrence and no observable effect on properties. One of the general trends reported in the literature is that transcrystalline layers tend to nucleate more readily in rapidly cooled specimens,[23] with the effect related to greater stresses generated between fiber and melt with less time to relax.[15] A contrary effect is also noticeable, in that transcrystalline layers formed at higher temperatures can grow farther because of less competition from spherulitic nucleation in the melt.[16] However, in the present specimens nucleation on the fibers that gives rise to transcrystalline layers is too sporadic to contribute much to or detract significantly from the mechanical properties. On occasion, regions are seen in which crystallization has occurred on row nuclei (Fig. 8), formed where the melt was stretched by handling during placement in the oven.[14]

## Differential Scanning Calorimetry

Differential scanning calorimetry is widely used to determine the degree of crystallinity in semicrystalline polymers. Values for this are plotted in Figure 9(a). Significantly, all specimens that were molten when removed from the oven and then

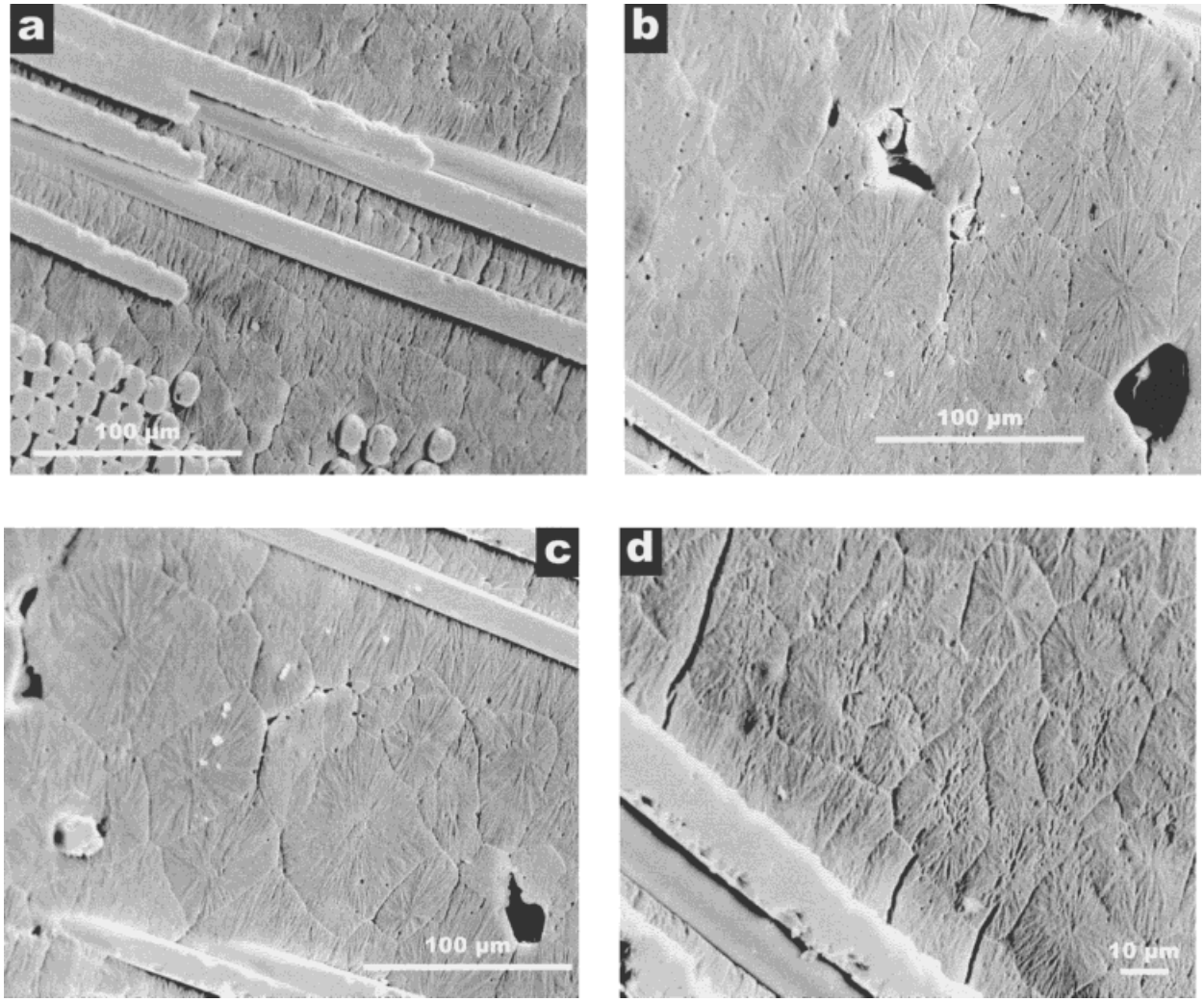


**Figure 6** SEM micrographs of specimens crystallized for 240 min at: (a) 106°C, (b) 115°C, (c) 125°C, and (d) 156°C.

were rapidly quenched are $\chi \sim 45\%$, while those crystallized in the oven show a steady increase from $\chi \sim 51\%$ for 106°C to $\chi \sim 60\%$ for 134°C. Peak melting points of individual runs are plotted in Figure 9(b). However, in regard to any attempt to obtain crystal thickness from melting points, reorganization during the scan is invariably a major feature and effectively transforms the melting endotherms of PP treated at crystallization temperatures of 125°C or below.[24] As a consequence, this technique cannot be expected to reveal much information relevant to morphology. However, in the 134°C specimens the DSC peak is observed to move from the region of 165°C at 10 min or 30 min (where the bulk of the specimen was still molten on removal from the oven) to 169°C after 1 h or 4 h, where crystallization was nearly or almost complete. One specimen, 134°C at 4 h, displayed a remarkably high melting point of 174°C. Here it is likely that the specimen was taken from a region that had a row nucleated and where the presence of the row nuclei allowed crystallization to take place at higher temperatures (while the specimen was still cooling in the oven).

### Impact Morphology

In spherulitic specimens there are different orders of junction between spherulites. Generally, a section through a surface will encounter a plane where two spherulites have met, and this will show as a line in the surface. Where three such lines meet at a point in the surface will be where three spherulites have interfaced. This has been called a *triangular junction* in a study of the morphology of consolidated ultrahigh-molecular-

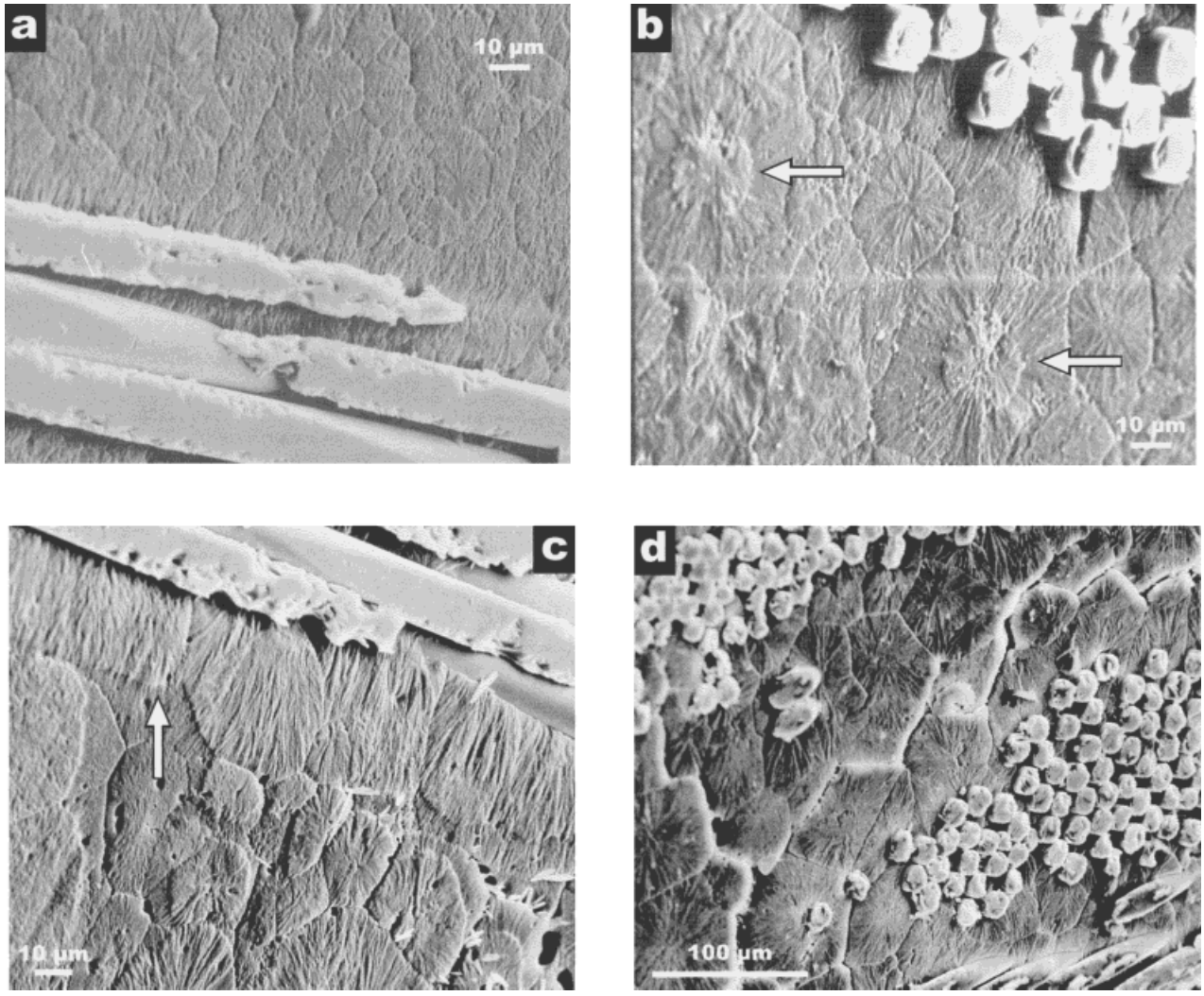


**Figure 7** SEM micrographs of specimens crystallized at 134°C at: (a) 10 min, (b) 30 min, (c) 60 min, and (d) 240 min.

weight polyethylene, as used in hip cups.[25] Occasionally, the surface will pass through the point where four spherulites have met at a *tetrahedral junction*. This is where voids are likely to form as space is filled with semicrystalline material, but solidification is still proceeding, and liquid is withdrawn into the spherulitic architecture.[26] It is unlikely that these instantaneously formed retraction voids are major causes of weakness, though they can be sites for electrical breakdown.[27] Moreover, most of the larger voids observed are probably a result of small air bubbles trapped in the specimens as the laminates were pressed together. However, further solidification occurs (with annealing) as the specimen is held at $T_c$ and the degree of crystallinity increases. This is likely to cause weakness at the plane junctions of the spherulites, exacerbated by this being the most likely site of the highest concentrations of uncrystallizable impurities. Failure along such spherulitic boundaries in an impacted 134°C 240-min specimen is shown in Figure 6(d). The area shown is several centimeters from the impact zone in a region where no damage is visible at low magnification.

Specimens crystallized for shorter durations develop small spherulitic structures with fewer interspherulitic defects or voids present, along with good bonding between glass fibers and transcrystalline layers. This makes the samples strong and less easily deformed. As a result, only very localized damage forms around impacted areas, as shown in Figure 10(a). This suggests fewer interspherulitic cracks occurred in the structure, and therefore less energy is associated with creating these cracks, that is, less energy has been

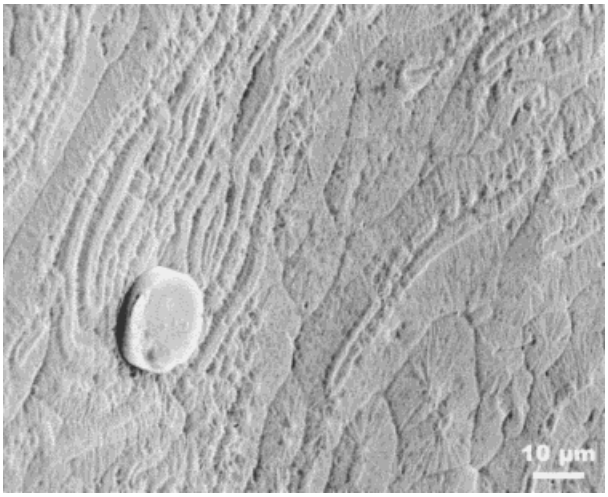


**Figure 8** SEM micrographs of a specimen crystallized at 106°C for 10 min, showing row structures in a region where the melt was stretched.

absorbed. For this reason the samples have low impact strength. The situation changes considerably with the 30-min specimens [Fig. 10(b)], in which crystallization has only just started to develop. Although the peak and failure energies are only a little higher than those of the 10-min specimens, considerable cracking has occurred. This may be aided by transcrystalline layers, which would be more heavily nucleated than the material comprising the bulk of the specimen and which would not be well bonded to the fibers. These are, however, much too localized in occurrence to contribute significantly to the value of the impact energy. The much greater weakness of the 134°C 240-min samples can be seen from extensive surface cracking [Fig. 10(c)] and the dome-type shape of the impacted zone, as shown in the transverse view in Figure 10(d). As already shown in Figure 7(d), the cracking extends through the interior of the specimen for a considerable distance from the impact zone.

## Failure Mechanism

Of the two processes by which fracture energy can be dissipated, two are of potential importance: creation of new surfaces and localized plastic deformation.[28] In the present work the greatest impact energy has also been found in specimens whose lamellar perfection is greatest. But although slower isothermal crystallization and/or subsequent annealing would increase lamellar perfection with a concomitant increase in tensile modulus, it would also be associated with a reduction in the occurrence of tie molecules. This would lead to a reduced propensity for plastic deformation at crack tips. Therefore, a gain in impact energy is sought in the greatly increased area of interspherulitic cracking. Reduction in tie molecules, segregation of impurities, and void formation at interspherulitic junctions all play their part in assisting this.

It has been noticed that in general slow crystallization and large spherulite size produce poor impact strength. Although there is a general correspondence between spherulite size in the 240-min specimens (Fig. 3) and impact energies (Fig. 4), it can be noted that the overall surface area of interspherulitic boundaries will actually be less when the spherulites are bigger. It is therefore in the quality of the material in these boundaries, rather than in the quantity, that an explanation is to be sought, as in one particular study, in which this effect is attributed to a changeover

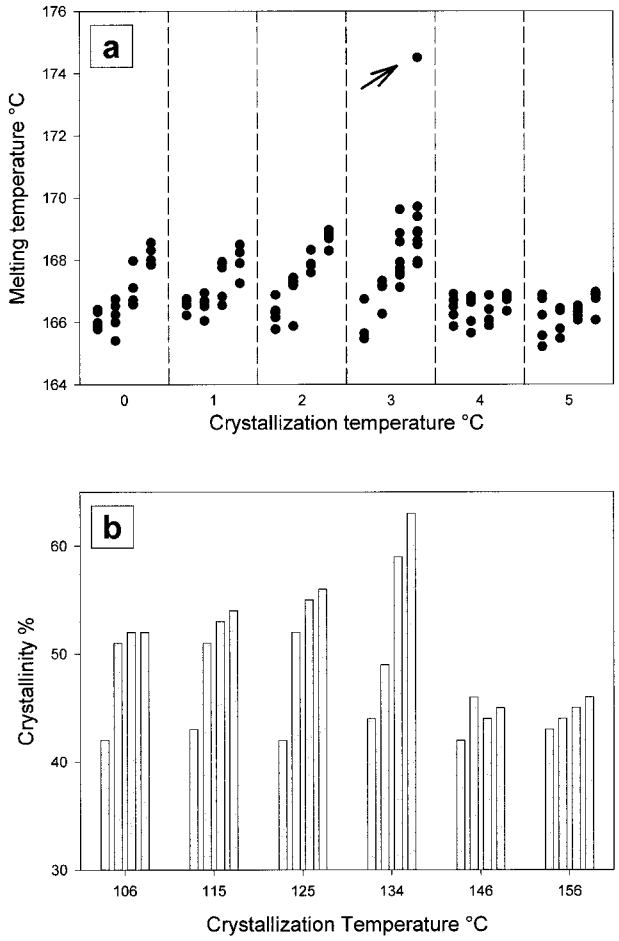


**Figure 9** DSC data for all specimens: (a) peak melting points from individual DSC runs, and (b) degree of crystallinity.

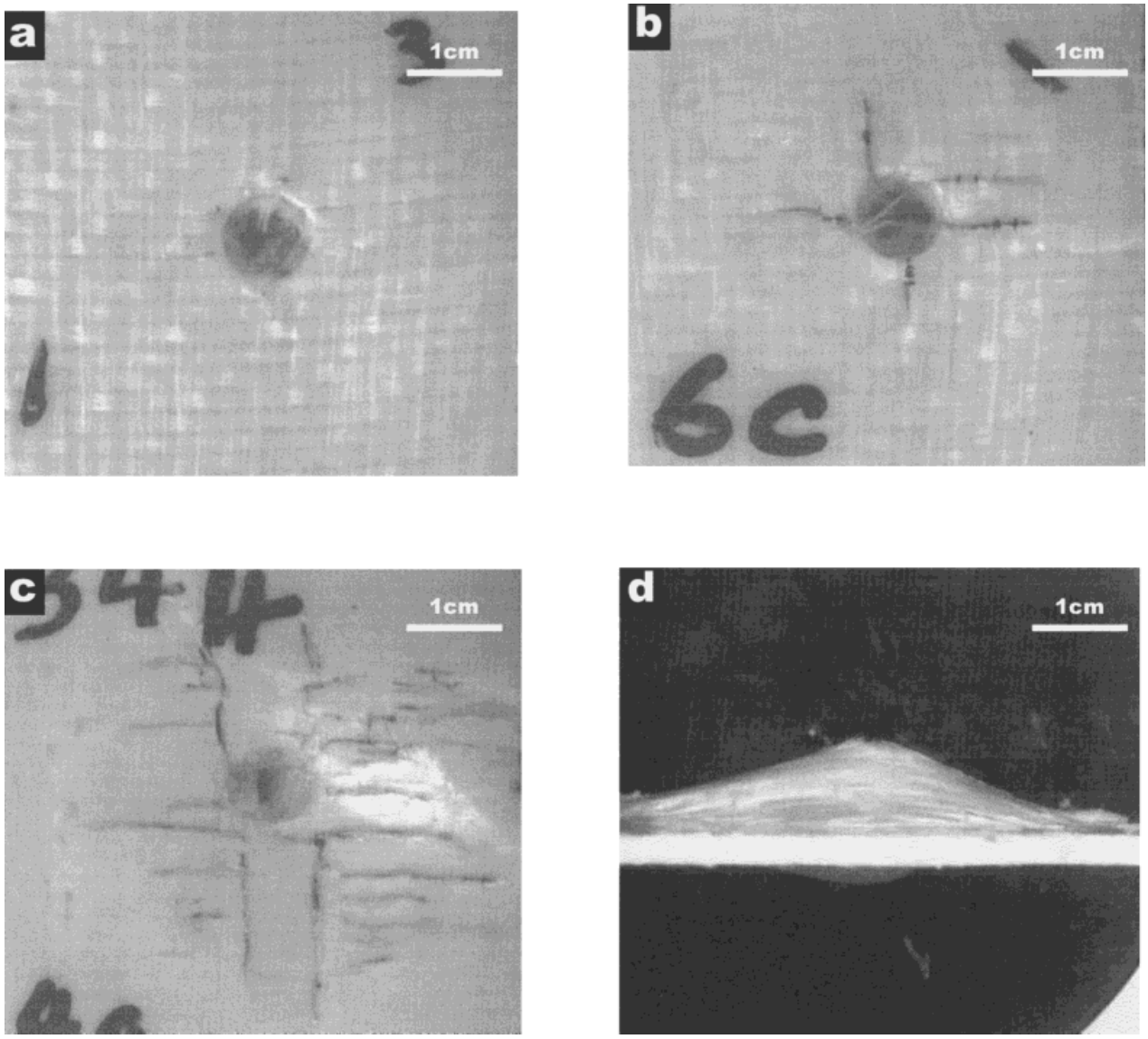


**Figure 10** Optical micrographs of impact tested specimens crystallized at 134°C at (a) 10 min, (b) 30 min, (c) 240 min, and (d) 240 min (side view).

from yielding within the spherulites in rapidly crystallized specimens to yielding at the boundaries between spherulites, brought about by increased segregation of impurities at the boundaries combined with void formation because of contraction of the spherulites on cooling.[7] The present work has extended these observations to conditions in the bulk of the material before total failure has occurred, and in particular, how this kind of failure mechanism can be turned to good account in the development of impact-resistant and shock-absorbing materials. Besides the presence of weak regions at the spherulitic boundaries, retraction voids tend to be abundant where transcrystalline layers boundaries impinge on the general spherulitic matrix. Another important factor is the interfacial bonding between the transcrystalline layers and the glass fibers. Heppenstall, Butler, and Young[17] found no significant link between morphological and stress variation, but did find significant variation between different thermal histories and the axial stress distribution along the glass fiber. They found that samples crystallized at higher temperature (producing coarser transcrystallinity) possess more uneven residual thermal-stress distribution than those crystallized at lower temperatures (producing fine crystallinity). This would lead to the 134°C samples possessing coarse and thick (about 50 $\mu$m) transcrystalline layers with relatively

poor interfacial bonding between glass fibers and transcrystalline layers.

Nevertheless, transcrystalline layers in the specimens are not frequent enough to dominate the failure mechanism, and the dominant factor in voidance at spherulitic boundaries is considered to be differential contraction of the glass and the polypropylene and of the crystalline and amorphous phases of the polypropylene.

A future work will investigate ways improving impact properties without having the long cycle times required by isothermal crystallization.

## CONCLUSIONS

- Electron microscopy of etched interior sections of woven glass fiber–reinforced polypropylene has enabled a more detailed understanding of the impact behavior of these materials.
- It is possible to improve significantly the impact energy of PP–glass fiber composites by crystallizing the polypropylene slowly, at a temperature of 134°C.
- Slow crystallization has the undesirable side effect of increasing cycle times to greater than 1 h.
- In such slowly crystallized specimens the effect of transcrystalline layers and their bonding to the fibers is of minor importance.
- Voids created within specimens by differential thermal-expansion effects play an important role in influencing impact performance.

The authors thank Dr. P. J. Isles of the Postgraduate Research Institute for Sedimentology, University of Reading, for his help with the scanning electron microscopy.

## REFERENCES

1. Lee, S. M. International Encyclopedia of Composites; VCH: New York, 1990; Vol. 5.
2. Hou, M.; Ye, L.; Mai, Y.-W. Plast, Rubber Compos Process Appl 1995, 23, 279.
3. Friedrich, K.; Hou, M. Comp Part A 1998, 29A, 217.
4. Bush, S. F.; Yilmaz, F.; Zhang, P. F. Plast Rubber Compos Proc Appl 1995, 24, 139.
5. Talbott, M. F.; Springer, G. S. J Compos Mater 1987, 21, 1056.
6. Way, J. L.; Atkinson, J. R. J Mater Sci 1971 , 6, 102.
7. Way, J. L.; Atkinson, J. R.; Nutting, J. J Mater Sci 1974, 9, 293.
8. Davies, P.; Cantwell, W. J. Composites 1994, 25, 869.
9. Ye, L.; Friedrich, K. J Mater Sci 1993, 28, 773.
10. Cantwell, W. J. J Compos Mater 1996, 30, 1266.
11. Varga, J.; Karger-Kocsis, J. J Compos Sci Technol 1993, 48, 191.
12. Moon, C. K. J Appl Polym Sci 1998, 67, 1191.
13. Thomason, J. L.; Van Rooyen, A. A. J Mater Sci 1992, 27, 889
14. White, H. M.; Bassett, D. C. Polymer 1997, 38, 5515.
15. Thomason, J. L.; Van Rooyen, A. A. J Mater Sci 1992, 27, 897.
16. Youssef, Y.; Denault, J. Polymer Composites, 1998, 19, 301.
17. Folkes, M. J.; Hardwick, S. T. J Mater Sci Lett 1987, 6, 656.
18. Olley, R. H.; Bassett, D. C. Polymer, 1982, 23, 1707.
19. Quirk, R. P.; Alsamarraie, M. A. A. In Polymer Handbook; Brandrup, J., Immergut, E. H., Eds.; Wiley & Sons: New York, 1989; p 29.
20. Wunderlich, B. Macromolecular Physics, Nucleation, Crystallization, Annealing; Academic Press: New York, 1976; Vol. 2.
21. McGenity, P. M.; Hooper, J. J.; Paynter, C. D.; Riley, A. M.; Nutbeem, C.; Elton, N. J.; Adams, J. M. Polymer 1992, 33, 5215.
22. Zok, F.; Shinozaki, M. D. J Mater Sci Lett 1994, 13, 940.
23. Yue, C. Y.; Cheng, W. L. J Mater Sci 1991, 26, 870.
24. Kim, Y. C.; Ahn, W.; Kim, C. Y. Polym Eng Sci 1997, 37, 1003.
25. Olley, R. H.; Hosier, I. L.; Bassett, D. C.; Smith, N. G. Biomaterials 1999, 20, 2037.
26. Galeski, A.; Piorkowska, E. J Polym Sci, Polym Phys Edn 1983, 21, 1313.
27. Galeski, A.; Piorkowska, E. J Polym Sci, Polym Phys Edn 1983, 21, 1299.
28. Young, R. J. In Comprehensive Polymer Science; Booth, C., Price, C., Eds.; Pergamon: Oxford, 1989; Vol. 2, Chapter 15, p 511.